

Optomechanical design concept for the Giant Magellan Telescope Multi-object Astronomical and Cosmological Spectrograph (GMACS)

Travis Prochaska^{*a}, Marcus Sauseda^a, James Beck^a, Luke Schmidt^a, Erika Cook^a, Darren L. DePoy^a, Jennifer L. Marshall^a, Rafael Ribeiro^b, Keith Taylor^c, Damien Jones^d, Cynthia Froning^e, Soojong Pak^f, Claudia Mendes de Oliveira^b, Casey Papovich^a, Tae-Geun Ji^f, Hye-In Lee^f

^aDepartment of Physics & Astronomy, Texas A&M University, 4242 TAMU, College Station, TX 77843-4242; ^bDepartamento de Astronomia, IAG, Universidade de São Paulo, Cidade Universitária, 05508-900, São Paulo, Brazil; ^cInstruments4, CA 91011, USA; ^dPrime Optics, Australia; Department of Astronomy, C1400, ^eUniversity of Texas at Austin, Austin, TX 78712; ^fSchool of Space Research, Kyung Hee Univeristy, Yongin-si, Gyeonggi-do 17104, Republic of Korea

ABSTRACT

We describe a preliminary conceptual optomechanical design for GMACS, a wide-field, multi-object, moderate-resolution optical spectrograph for the Giant Magellan Telescope (GMT). This paper describes the details of the GMACS optomechanical conceptual design, including the requirements and considerations leading to the design, mechanisms, optical mounts, and predicted flexure performance.

Keywords: multi-object spectrograph, camera, CCD, VPH grating, Giant Magellan Telescope

1. INTRODUCTION

This paper presents the preliminary conceptual optomechanical design of the wide field, multi-object, moderate-resolution, optical spectrograph, called GMACS. GMACS (Giant Magellan Telescope Multi-object Astronomical and Cosmological Spectrograph) is a first light instrument for the Giant Magellan Telescope (GMT)^[1]. Figure 1 illustrates where the instrument is located at the Gregorian focus of the GMT. GMACS is an instrument capable of observing the faintest possible targets, those that are substantially fainter than the sky. High throughput, simultaneous wide wavelength coverage, accurate and precise sky subtraction, moderate resolution, and wide field are the crucial design drivers for the instrument. We expect that GMACS will form one of the most basic scientific capabilities of the GMT.

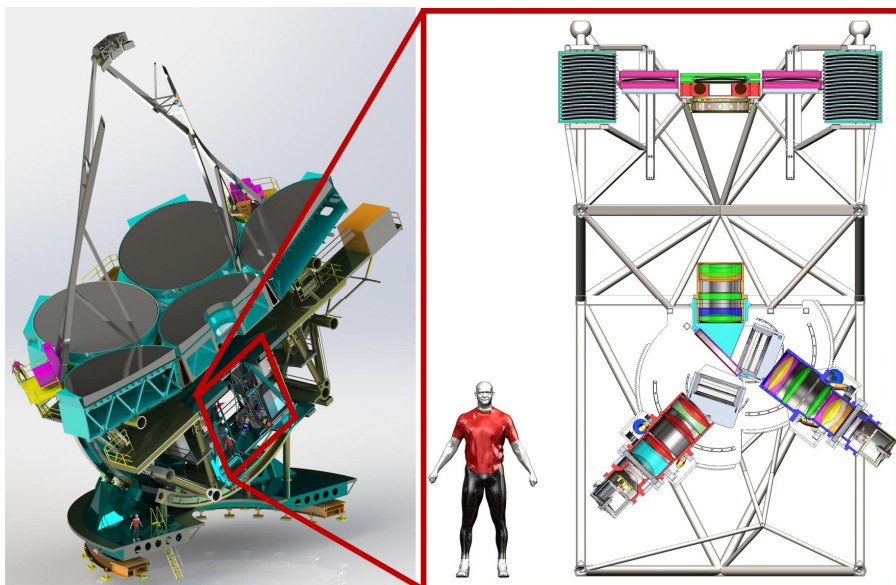


Figure 1. Location of the GMACS instrument within GMT.

* tprochaska@physics.tamu.edu; Phone 1-979-862-2747; <http://instrumentation.tamu.edu/>

The optical performance specifications for GMACS have been developed through collaboration with GMTO, partner institutions and members of the scientific community. The minimum specifications are listed in Table 1 along with stricter specifications we hope to achieve. More details on the preliminary conceptual optical design^[2] can be found in SPIE paper 9908-376.

Table 1. List of GMACS functional specifications.

Parameter	Requirement	Goal
Field of View	30 arcmin sq.	50 arcmin sq.
Wavelength Coverage	350-950nm	320-1000nm
Spectral Resolution	Blue: 1000-6000, Red 1000-6000	Blue: 1000-6000, Red 1000-6000
Image Quality	80% EE at 0.30 arcsec	80% EE at 0.15 arcsec
Spectral Stability	0.3 spectral resolution elements/hour	0.1 spectral resolution elements/hour
Number of Gratings	2	≥ 2
Slit Mask Exchange	12	≥ 20

The current GMACS design is a new preliminary concept, evolving from the 2012 conceptual design^[3], while scaling its size down to meet budgetary constraints. The scope of the preliminary conceptual optomechanical design is to illustrate how the optics and subsystems will be packaged, to simulate articulation ranges of the moving components and identify potential collisions, estimate initial instrument envelope and weight (Figure 2), investigate GMT interfacing, and determine expected deformations. Much of this will be used to feed back to the optical design's development. In future iterations, we will also investigate our interface with MANIFEST, the "starbug" fiber positioning system^[4], which is discussed in SPIE paper 9908-358.

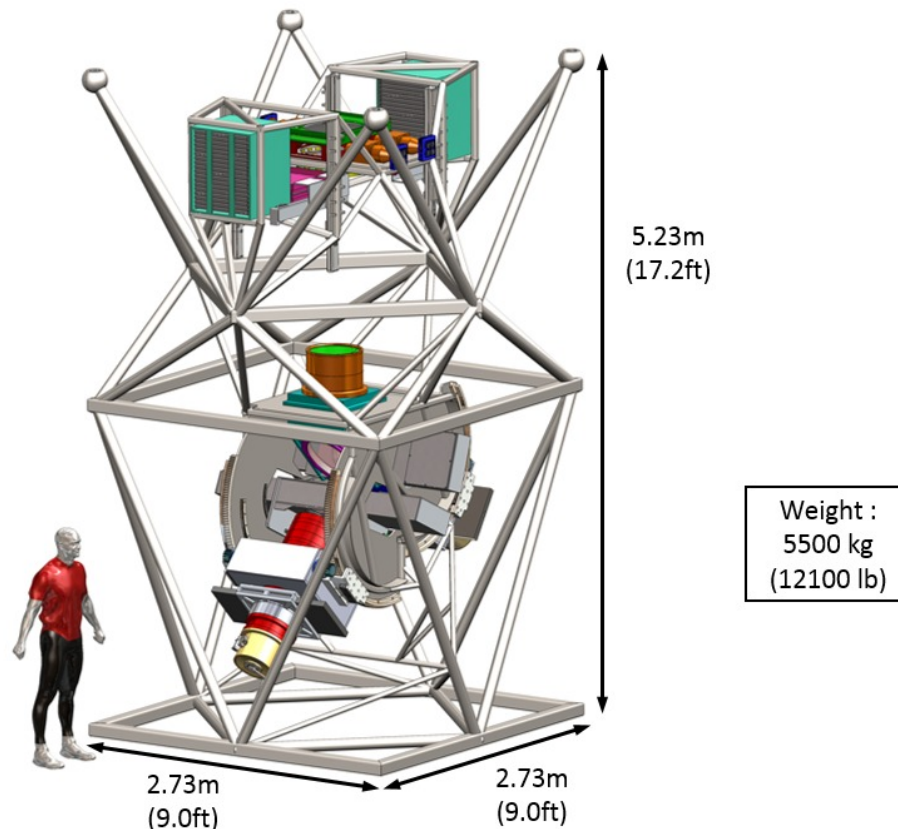


Figure 2. Overall size and weight of GMACS.

2. INSTRUMENT MOUNTING

2.1 Frame

GMACS's current frame design (Figure 3) is a tubular spaceframe structure that will hold the instrument subassemblies together and attach the instrument to the back of the GMT. The spaceframe style will be very stiff and will help evenly distribute the instrument load to the GMT mechanical interface. The frame will be relatively straightforward to fabricate and weld with a proper fixturing system. The frame will be made of steel for its strength, stiffness, availability, machinability, weldability and cost. The design of this system is still being optimized to reduce mass and simplify the load paths.

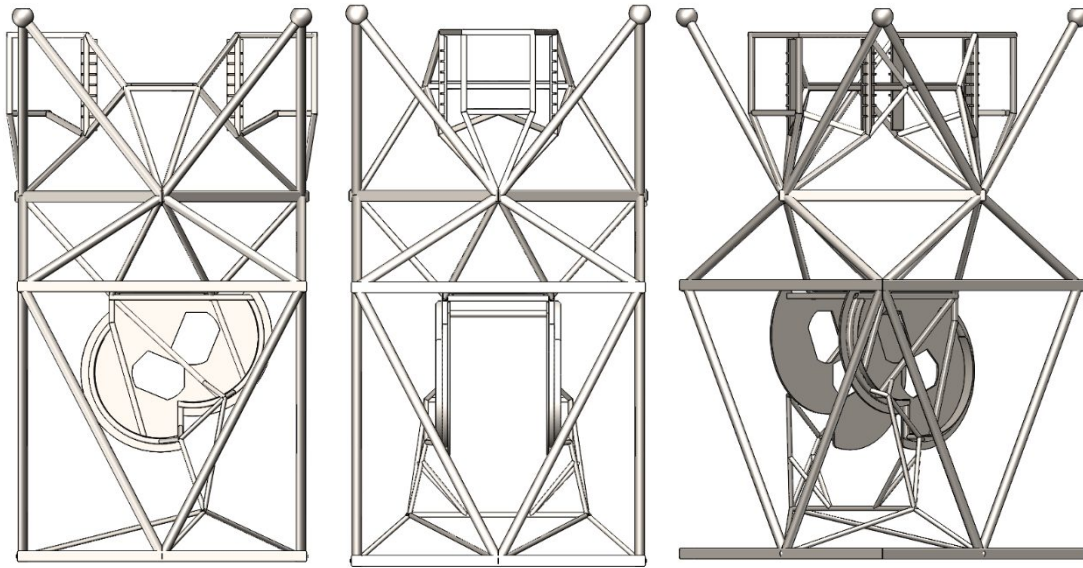


Figure 3. Front, side and diagonal view of the GMACS spaceframe structure.

The frame will completely outline much of the instrument subsystems, allow the instrument to be placed on the frame's bottom, front or back side for assembly, storage, shipping, and maintenance. This reduces the need for a specialized instrument cart to be used at all times during the instrument development process. The frame will also be used as a natural attachment structure for all the side paneling to form the environmental enclosure to keep out stray light and foreign objects and to stabilize the internal temperature.

2.2 GMT Mechanical Interface

The GMT mechanical interface will enable GMACS and other instruments to attach to the back of the telescope at the Gregorian focus. This interface will also de-rotate the instrument to track the field. In the 2012 GMACS design, the GIR (Gregorian Instrument Rotator) was used to interface with the instrument. This system would also store and engage instruments automatically. The current GMACS design will be demonstrating a sphere and cone system that could be used as an alternative attachment method. This technique is similar to the one used on the MODS instrument^[5] at the Large Binocular Telescope. Ultimately, the current frame is modular enough to easily switch between different mounting schemes if needed.

3. FOCAL PLANE ASSEMBLY

The focal plane assembly sits on the top quarter section on the instrument frame. This section contains the field lens, guide & acquisition camera and the slit mask exchange mechanism, as seen in Figure 4. These systems are described in more detail in the following sections.

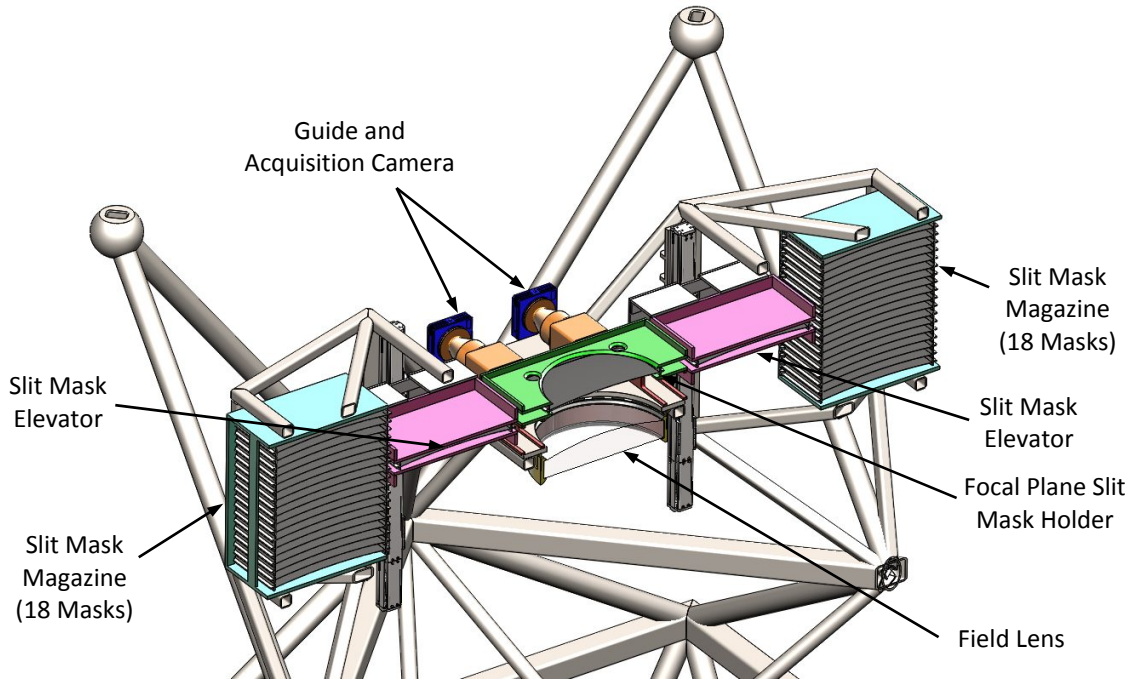


Figure 4. Section view of the focal plane assembly.

3.1 Field Lens

The field lens is the first and largest optic in our system. It is a 520mm diameter silica lens and weighs 46kg. We plan to adapt a cell design similar to the one used in the DECam instrument^[6] and in the MMT's wide field corrector^[7] since these design have proven to work well for large lenses. To account for differentials in the coefficient of thermal expansion (CTE), this design utilizes invar cells with room temperature vulcanization (RTV) pads to hold the lens and flexures to attach the cell to the steel frame. Our concept is shown in Figure 5.

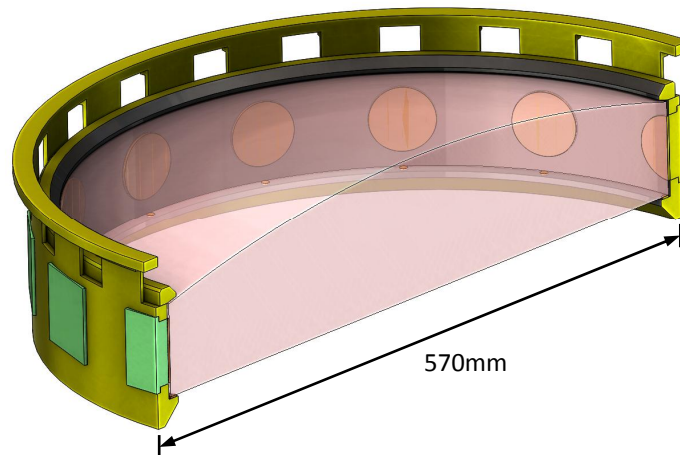


Figure 5. Section view of the field lens in its cell.

3.2 Guide and Acquisition Camera

The focal plane assembly will carry four alignment and acquisition cameras as seen in Figure 6. These cameras are in a fixed location behind the focal plane each having ~ 1 arcminute field of view. The acquisition and alignment cameras will be in fixed locations behind reference holes cut in every slit mask. They will allow precision alignment of the slit masks relative to reference stars that can be positioned appropriately on the CCDs. The density of reference objects on the sky should be very high, since the GMT can quickly detect extremely faint objects.

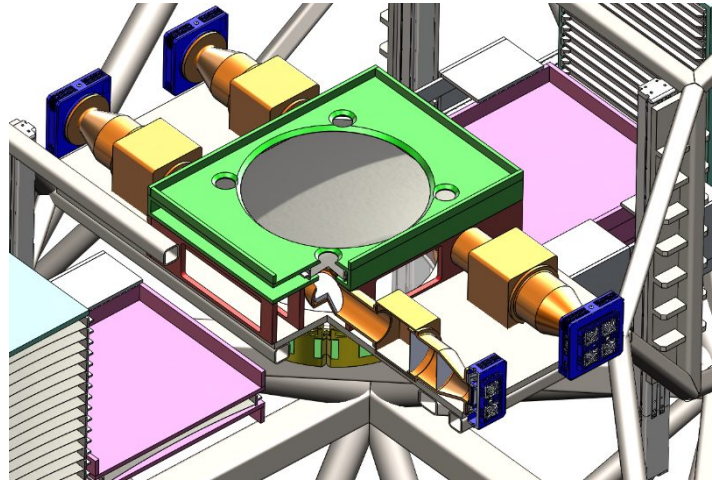


Figure 6. Slit mask focal plane holder with the 4 guide and acquisition cameras.

In future designs, one of the alignment and acquisition cameras may be replaced by another camera on a multi-axis rail system. This camera can be robotically positioned under slits to verify the alignment with its target on the sky. We will also investigate another technique to do the slit mask alignment using the actual GMACS red and blue cameras. By rotating the cameras and gratings to be on axis, the red and blue cameras can take an image of the slit mask and targets to verify the alignment.

3.3 Slit Mask Exchange Mechanism

In order to observe multiple objects in many different fields throughout the night, a jukebox style exchange mechanism will be used to move various slit masks into the focal plane and back into a storage magazine. The slit masks are 500 mm x 500 mm in size. Currently each mask will be held in a cartridge that is 521 mm x 540 mm x 31 mm and will be curved to follow the best focal surface of the telescope, as shown in Figure 7. The cartridge will use rails and rollers to translate into the storage magazine, elevator and focal plane observing locations. While in the focal plane holder, a slit mask is captured kinematically and will be held in place with a stability of ~ 10 microns.



Figure 7. Concept of the GMACS slit mask in its cartridge.

To keep the slit mask from being over constrained, the magazines use vee groove guide wheels on the left side and crowned rollers on the right. In addition, the upper wheels and rollers will be on flexures that allow them to adjust for varying rail separations. While translating in and out of the elevator, the tracks will remain in contact with at least 2 pairs of guide wheels at any time. Examples of these roller are shown in Figure 8.



Figure 8. Commercial off-the-shelf vee groove guide wheels and crowned rollers^[8] that could be used to precisely move and hold the GMACS slit masks.

In the exchange mechanism, the slit mask elevator moves the slit masks from the magazine to the observing position. The system uses four linear actuators (THK, Universal Series) to securely move the slit mask from the magazine to the focal plane. A horizontal linear actuator extracts the mask from the magazine, and two vertical linear actuators raise the mask to the height of the focal plane where the mask is inserted into the focal plane holder with the same horizontal linear actuator. Both can be seen in Figure 9. The last linear actuator uses a linkage system to engage a detent on the mask cartridge while riding on the horizontal linear actuator, as seen in Figure 10.

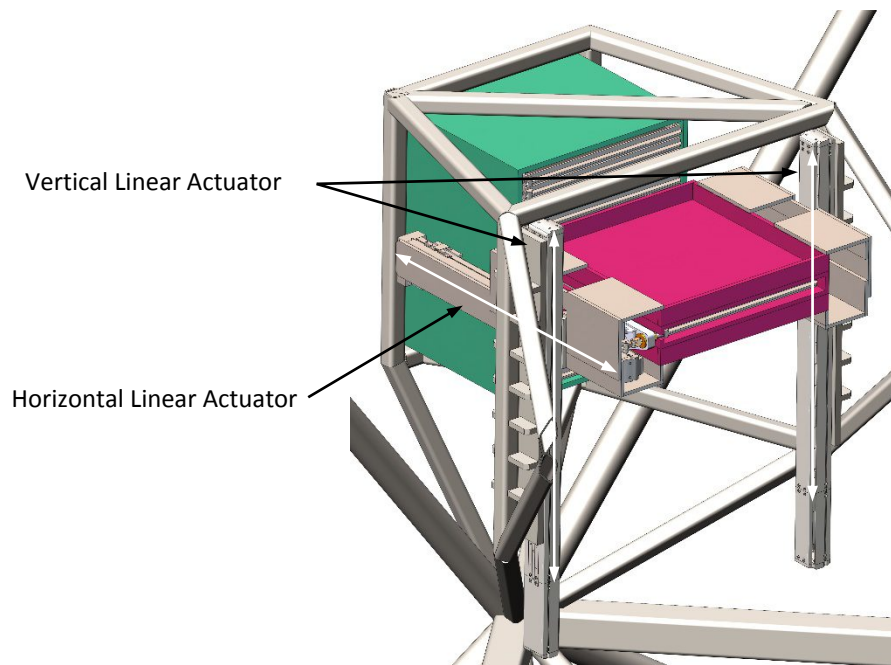


Figure 9. Vertical & horizontal linear actuators that are used in the slit mask elevator system.

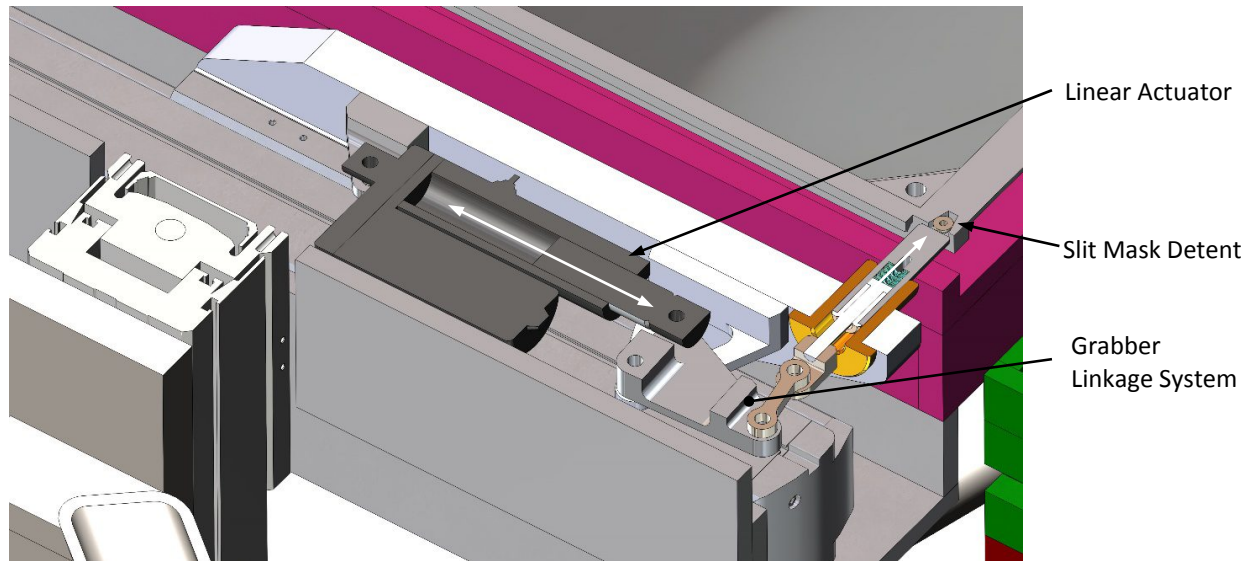


Figure 10. Section view of the slit mask grabbing system.

There is currently enough space on the focal plane assembly for two slit mask exchange mechanisms that will share the same focal plane holder. Having two slit mask exchange mechanisms will obviously double the quantity of usable slit masks per night, but more importantly will allow the spectrograph to remain operational if one slit mask exchange mechanism breaks down. Each slit mask magazine can hold 18 slit masks for a total of 36 slit masks.

4. OPTICS MODULE

The optics module contains a majority of the optics and sits in the lower half of the instrument frame. This section contains the collimator, dichroic, gratings and cameras as seen in Figure 11. It also contains systems that independently articulate and hold the cameras and gratings at various angles. This is to accommodate multiple grating resolutions. In low resolution mode ($R \sim 1000$) and high resolution mode ($R \sim 6000$) the collimator-camera angle must be $\sim 18.2^\circ$ and $\sim 88.9^\circ$, respectively. This and the other optics module systems are described in more detail in the following sections.

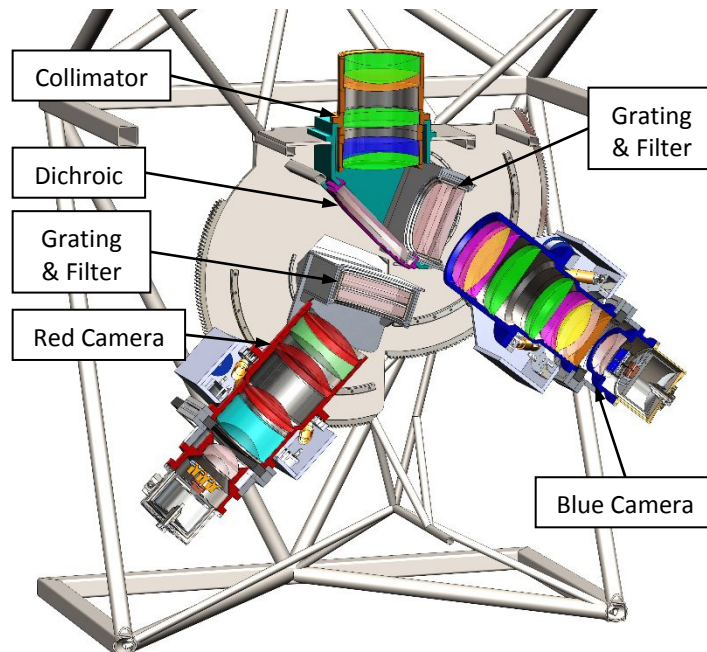


Figure 11. Section view of the GMACS optics module's primary subsystems.

4.1 Collimator, Dichroic and Cameras

The lens cell concepts for the collimator, dichroic and cameras optomechanical systems currently do not show precisely how they hold the optics, but the future design will be based on the cells used in the FourStar infrared camera^[9] and the SDSS spectrographs^[10], which are known to work well. These cells will use roller pin flexures and glass filled Teflon plugs to hold the lenses in alignment over varying temperatures. Figure 12, Figure 13 and Figure 14 below show the current details of the collimator assembly, blue camera, and red camera, respectively. Each camera will also have a Bonn shutter^[11] before the detector window to control the exposure time on each channel.

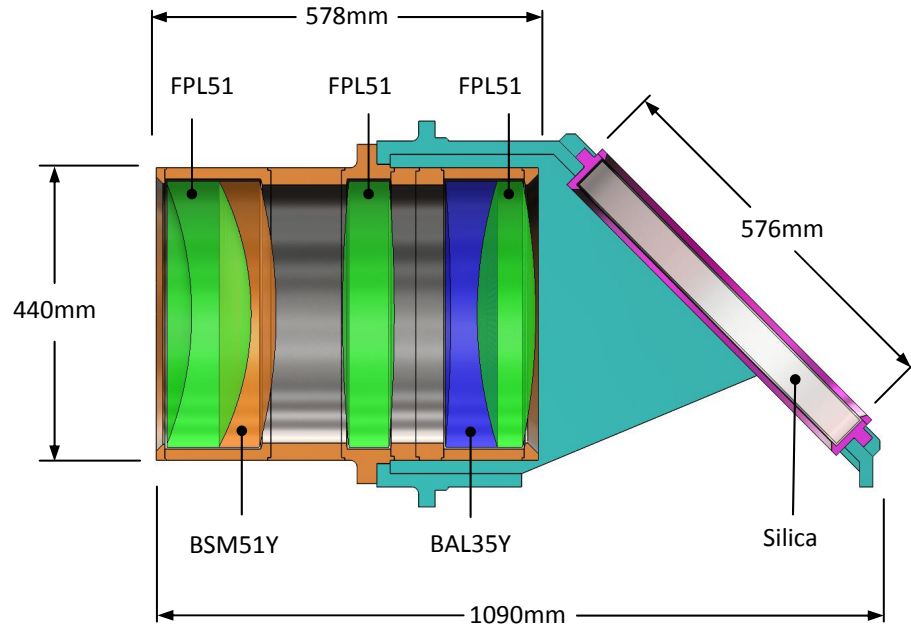


Figure 12. Section view of the collimator assembly with the dichroic beam splitter attached.

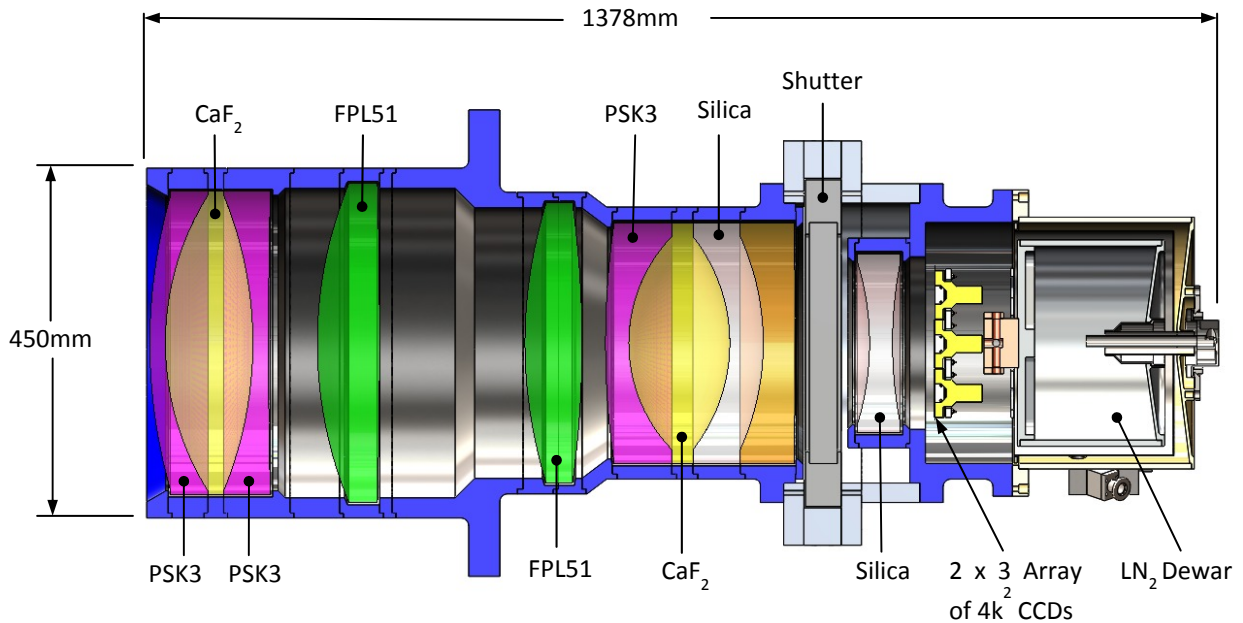


Figure 13. Section view of the blue camera showing the lens arrangement, cells, shutter, CCD and its cryostat.

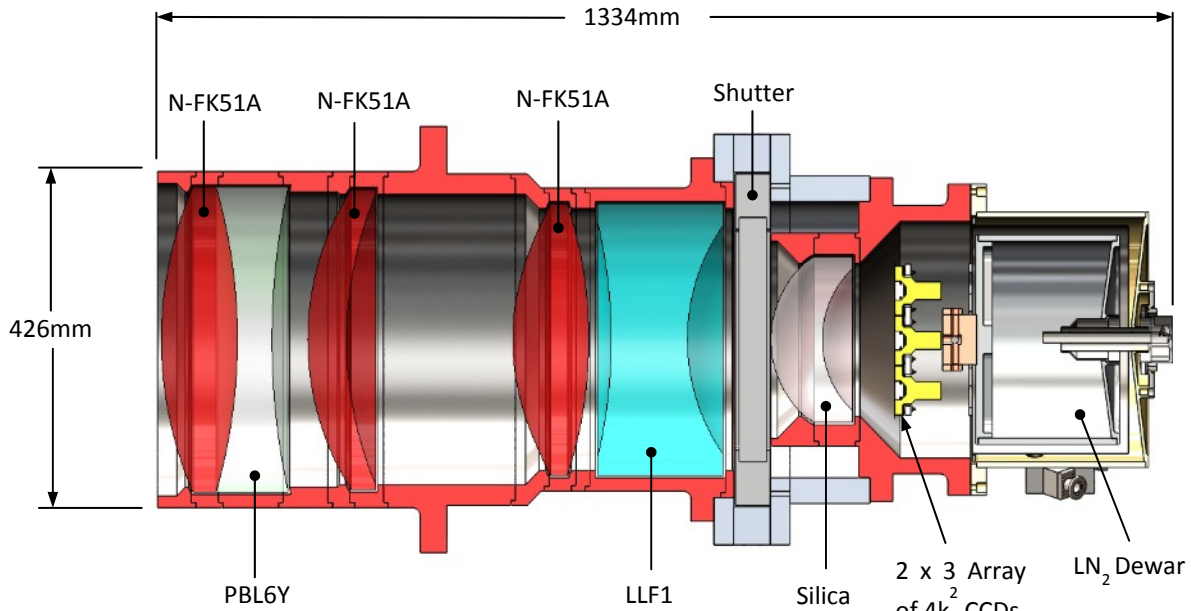


Figure 14. Section view of the red camera showing the lens arrangement, cells, shutter, CCD and its cryostat.

4.1.1 Camera Articulation

Each red and blue camera rotates $\sim 90^\circ$ on two sets of THK curved rails (model #: HCR35A+60 600R) attached to the internal faces of the mount plates, as seen in Figure 15. To rotate a camera on its rails, two Dual Harmonic Drive AC servo actuators (model SHA 40A 161) with brake, drive six pitch spur gears against mating arc gears. One drive is linked to the torque of the other for even loading. Each arc gear will have a pneumatic rail brake, which will lock the camera position allowing any orientation to be achieved within the limits of travel. This eliminates the concerns about effects of gear lash on deflection. Limit switches set the range of motion and additional limit switches prevent red/blue collision. There will also be hard stops to prevent over-travel. Concepts for motor, gears and brake are shown in Figure 16.

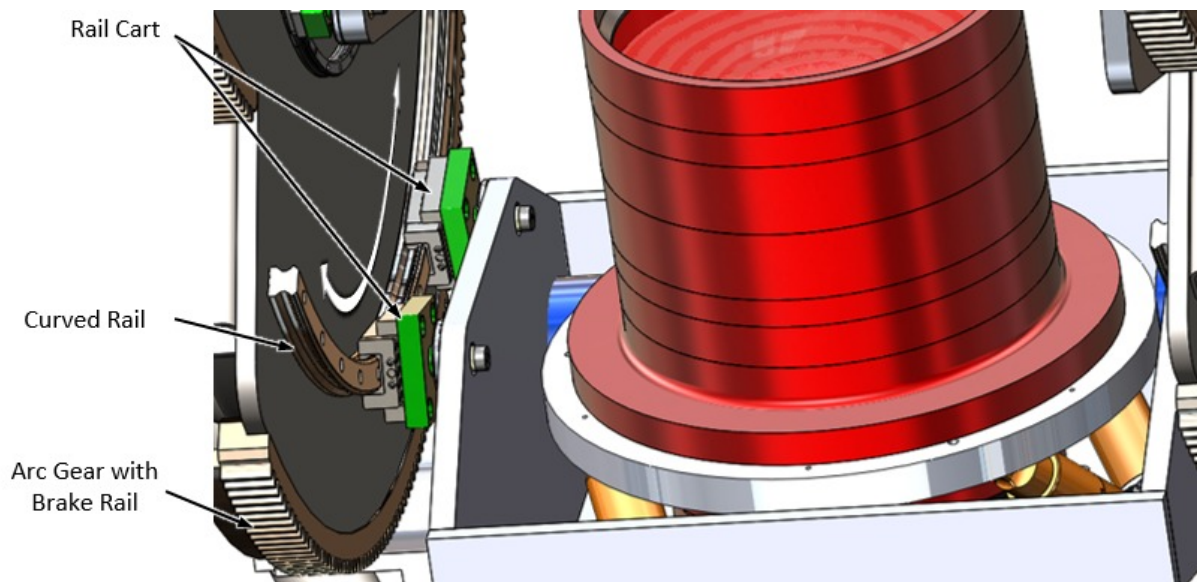


Figure 15. Camera rotation system.

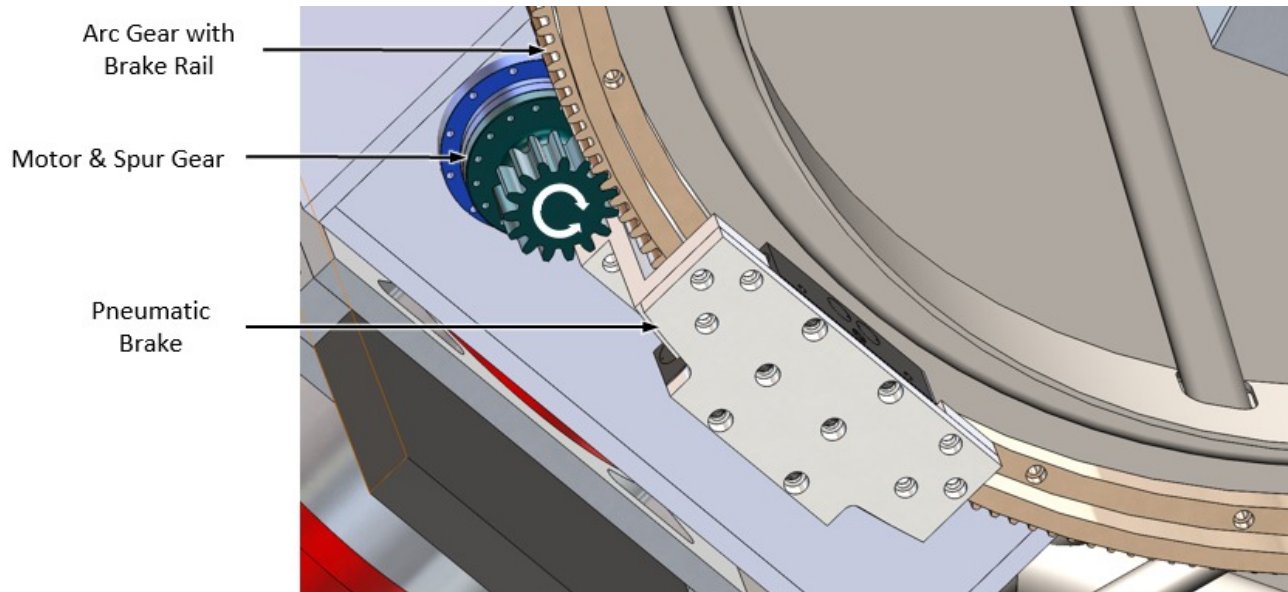


Figure 16. Motor and brake system used to move and hold a camera in various orientations relative to each grating.

4.1.2 Detector & Dewar

A cryostat holds the detector mosaic for each camera. The detector assembly will be formed by a 2x3 mosaic of $4k^2$ detectors with a pixel pitch of $15\mu\text{m}$. An example detector array is shown in Figure 17. We currently plan to use liquid nitrogen cooling for the detectors. Some thought has also been put into using cryo-coolers, but reliability and excess waste heat are a concern. A future trade study will examine possible cooling mechanisms, the cooling requirements of GMACS, and the GMT facility standards to make the final determination.

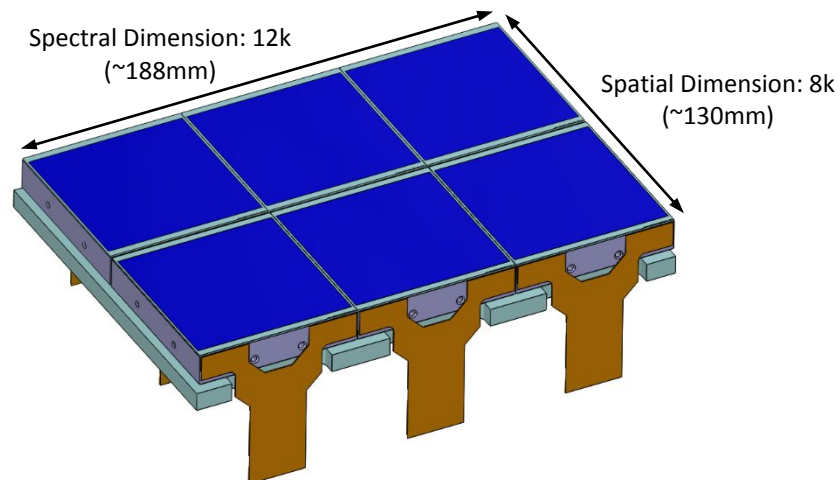


Figure 17. 2x3 CCD mosaic made from $4k^2$, $15\mu\text{m}$ detectors.

4.2 Grating & Filter Exchange Mechanism

The grating exchange mechanism is only required to hold two gratings, but a third position has been added to leave room for future expansion, for example to accommodate an additional medium resolution grating. Figure 18 below shows how the three gratings will be positioned in a row and can translate into different positions. One filter is located directly behind the grating and will move in & out of the light path as well.

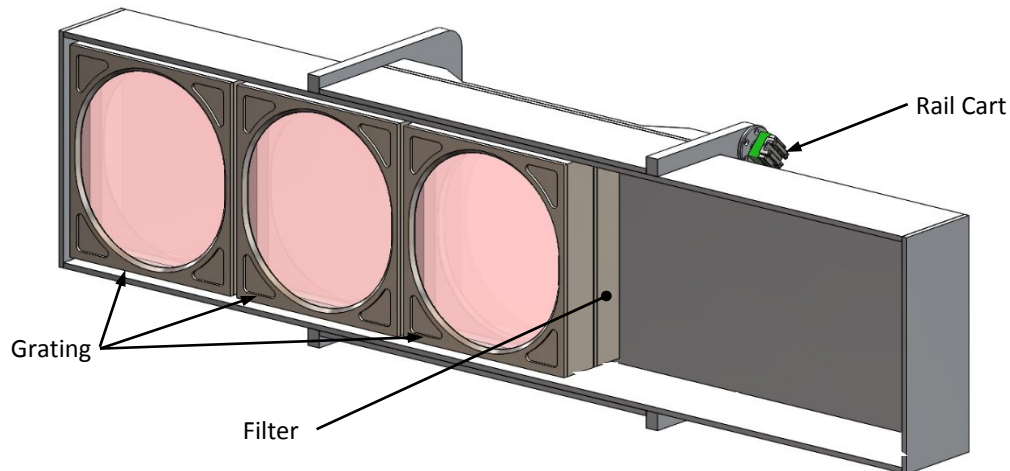


Figure 18. Opened view of the grating & filter exchange mechanism.

4.2.1 Grating & Filter Turret Rotation

The grating/filter turret rotates on two sets of THK curved rails (model #: HCR15A+60 300R) on the inside face of each base plate. Its rotation range will be $\sim 45^\circ$. Rotation is driven by a cylindrical linear actuator which provides simple backlash free motion. Encoding is not yet finalized, but options include linear potentiometer (baseline), an encoder on the rails, or simple open loop operation.

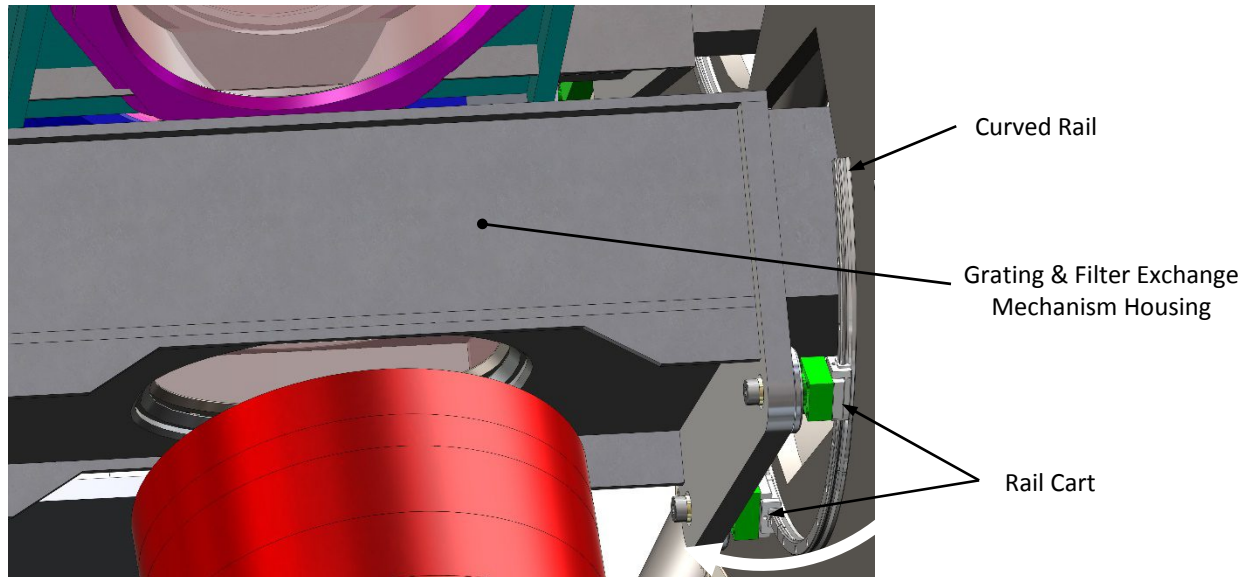


Figure 19. Grating & filter rotation system used to align each grating to the optical axis depending on its resolution.

4.2.2 Grating & Filter Exchange Mechanism

The grating and filter slide drive works with two sets of vee groove guide wheels that ride on parallel tracks to provide the requisite linear motion. The motive force is provided by a belt drive system, while limit switches set range of motion and hard stops preclude over-travel. The set of gratings will be able to translate 750mm (~ 29.5 in).

5. FLEXURE

Gravity-induced image motion is a common issue for spectrographs mounted at the Gregorian or Cassegrain focus of a large telescope. As the telescope tracks the sky, the gravity vector changes relative to the instrument. Hence, gravity-induced deflections within the spectrograph structure change over time, and alter the position and orientation of the optical elements housed within the structure. These subtle shifts of the optics translate into degradation and motion of the focused images at the camera detector focal plane, which ultimately reduces resolution and spectral stability. This problem is particularly acute for large instruments.

To help understand how gravity-induced deflections will affect our system, preliminary simulations have been set up to estimate the expected deflections. With these numbers, we hope to determine how much compensation will be required along with areas that will need to be stiffened or lightened. In future studies, we plan to feed these deformation values into the ZEMAX optical tolerance analysis and determine the impact to the spectrograph's optical performance at different gravity vectors.

5.1 Simulation

SolidWorks Simulation was utilized to setup and run an FEA to find the expected deflection. To expedite this process, many of the complex shaped parts were simplified into blocks and cylinders or turned into remote masses. This technique greatly reduces the meshing and calculation time without sacrificing much accuracy. Figure 20 shows the mesh of the simplified model.

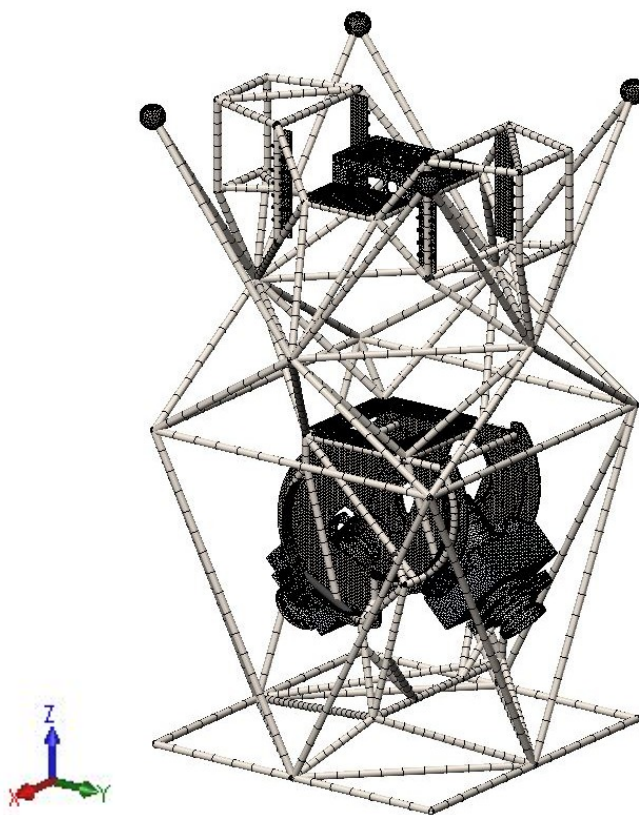


Figure 20. Meshed simplified version of GMACS with the instrument coordinate system.

For the preliminary tests, we wanted to determine how the red and blue focal planes would move while tracking the sky. To do this, the simulation was run at the largest angle the telescope will point relative to zenith (0°), which is 60° about the X axis and 60° about the Y axis. One last simulation was run at zenith as a reference. Figure 21, Figure 22 and Figure 23 illustrate GMACS's resultant displacement at the tested orientations, and Table 2 lists how the gravity-induced deflections will affect the focal planes. Figure 24 shows the coordinate system set up for the table.

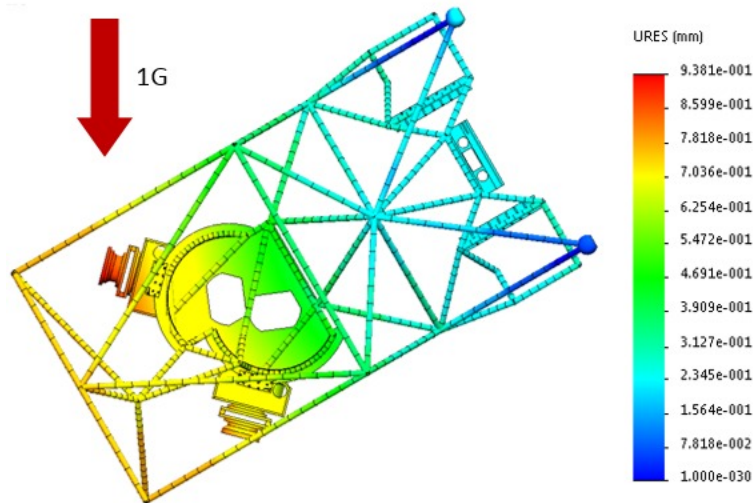


Figure 21. Resultant displacement of GMACS when it is rotated 60° about the X axis.

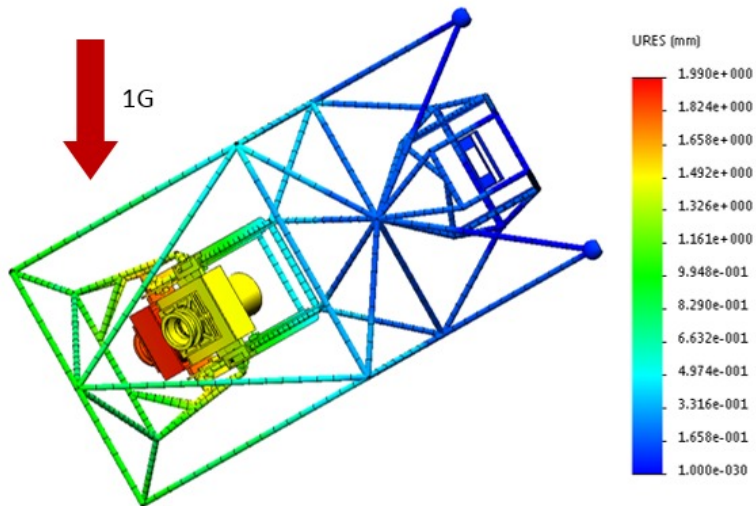


Figure 22. Resultant displacement of GMACS when it is rotated 60° about the Y axis.

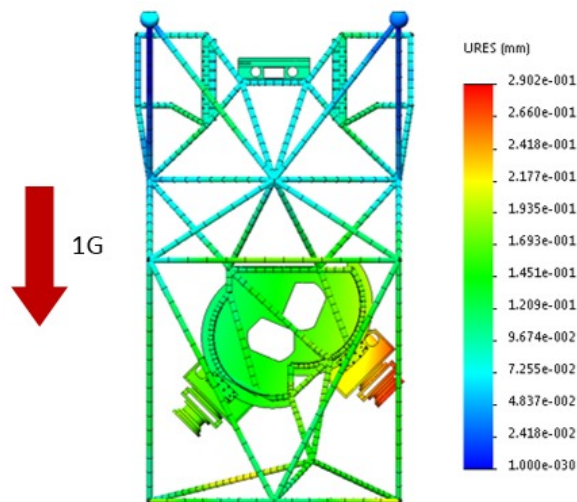


Figure 23. Resultant displacement of GMACS when it is pointing at zenith (0°).

Table 2. Results of the preliminary FEA used to find the deflection of each camera focal plane at various instrument orientations.

Instrument Orientation	Red Camera CCD						Blue Camera CCD					
	X Shift Spatial	Y Shift Spectral	Z shift Focal	θ_x	θ_y	θ_z	X Shift Spatial	Y Shift Spectral	Z shift Focal	θ_x	θ_y	θ_z
	(mm)	(mm)	(mm)	(°)	(°)	(°)	(mm)	(mm)	(mm)	(°)	(°)	(°)
60° about X	-0.074	0.833	0.383	0.000	0.017	0.000	-0.031	0.680	-0.410	0.014	0.002	0.002
60° about Y	-1.759	0.008	-0.072	0.000	0.375	0.008	-1.457	-0.154	-0.084	0.005	0.006	0.006
Zenith (0°)	0.044	0.085	-0.149	0.000	0.041	0.001	-0.026	-0.248	-0.127	0.006	0.001	0.001

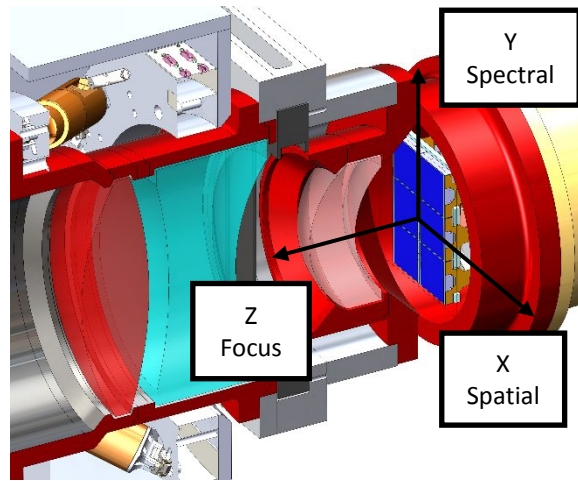


Figure 24. Coordinate system of the camera CCD used in the setup of the deflection simulation.

5.2 Compensation

To compensate for the expected deflection a hexapod will be used in a closed loop system to orient each camera into its optimal position. Our current flexure compensation strategy is to send laser beams through the system and measure where they land on quad-cells near the focal plane to track the cameras' relative positions. The laser beam wavelength will be outside the science wavelengths to avoid contaminating the data. Figure 25 shows the blue camera mounted to a hexapod made by Physik Instrumente. This hexapod is expected to translate the camera $\pm 2.5\text{mm}$, $\pm 2.5\text{mm}$ & $\pm 0.5\text{mm}$ in X, Y and Z, respectively, and rotate it $\pm 0.5^\circ$ in tip, tilt and clock. From Table 2, the hexapod specifications should meet the required compensation amounts, but we will continue to investigate ways to reduce deflections.

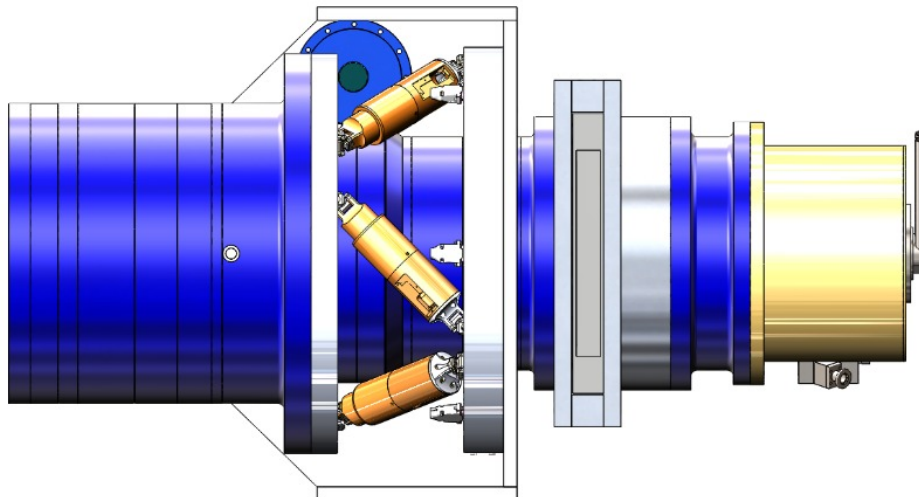


Figure 25. Hexapod used to compensate for gravity induced deflections.

6. CONCLUSIONS

GMACS's current conceptual design is still underway, but we have made significant progress advancing the design from the 2012 concept. In our models we have designed packages for the optics, a spaceframe structure to transfer the instrument load to the GMT, mechanisms to exchange slit masks and gratings, and articulation systems to rotate the cameras and gratings. Simulations on GMACS's gravity-induced deflections have shown we are in range of the hexapod compensation system. Everything is on track for the current conceptual design, but most subsystems still require additional refinement.

ACKNOWLEDGEMENTS

Texas A&M University thanks Charles R. and Judith G. Munnerlyn, George P. and Cynthia W. Mitchell, and their families for their support of astronomical instrumentation activities in the Department of Physics and Astronomy.

REFERENCES

- [1] DePoy, D. L., Marshall, J. L., Cook, E., Froning, C. S., Ji, T., Jones, D. J., Lee, H., Mendes de Oliveira, C., Pak, S., Papovich, C., Prochaska, T., Ribeiro, R., Schmidt, L. M., Taylor, K., "The Giant Magellan Telescope multi-object astronomical and cosmological spectrograph (GMACS)," Proc. SPIE 9908, Ground-based and Airborne Instrumentation for Astronomy VI, 990879 (2016).
- [2] Schmidt, L., Ribeiro, R., Taylor, K., Jones, D., Prochaska, T., DePoy, D. L., Marshall, J. L., Cook, E., Froning, C. S., Ji, T., Lee, H., Mendes de Oliveira, C., Pak, S., Papovich, C., "Optical design concept for the Giant Magellan Telescope Multi-object Astronomical and Cosmological Spectrograph (GMACS)" Proc. SPIE 9908, (2016)
- [3] Smee, S. A., Prochaska, T., Shectman, S. A., Hammond, R. P., Barkhouser, R. H., DePoy, D. L., Marshall, J. L., "Optomechanical design concept for GMACS: a wide-field multi-object moderate resolution optical spectrograph for the Giant Magellan Telescope (GMT)," Proc. SPIE 8446, Ground-based and Airborne Instrumentation for Astronomy IV, (2012).
- [4] Lawrence, J. S., Ben-Ami, S., Brown, D. M., Brown, R., Case, S., Chapman, S., Churilov, V., Colless, M., Content, R., DePoy, D. L., Evans, I., Goodwin, M., Jacoby, G., Klauser, U., Kuehn, K., Lorente, N. P. F., Mali, S., Marshall, J. L., Muller, R., Nichani, V., Pai, N., Prochaska, T., Saunders, W., Schmidt, L., Shortridge, K., Staszak, N. F., Szentgyorgyi, A., Tims, J., Vuong, M., Waller, L., Zhelem, R. "The MANIFEST Prototyping Design Study," Proc. SPIE 9908, (2016)
- [5] Pogge, R. W., Atwood, B., Brewer, D. F., Byard, P. L., Derwent, M. A., Gonzalez, R., Martini, P., Mason, J. A., O'Brien, T. P., Osmer, P. S., Pappalardo, D. P., Steinbrecher, D. P., Teiga, E. J., Zhelem, R. "The multi-object double spectrographs for the Large Binocular Telescope," Proc. SPIE 7735, Ground-based and Airborne Instrumentation for Astronomy III, (2010).
- [6] Doel, P. ; Brooks, D. ; Antonik, M. L. ; Flaughner, B. L. ; Stefanik, A. ; Kent, S. M. ; Gutierrez, G. ; Cease, H. P. ; Abbott, T. M. ; Walker, A. R. ; DePoy, D. L. ; Bernstein, R. A. ; Worswick, S. " Assembly, alignment, and testing of the DECam wide field corrector optics," Proc. SPIE 8446, Ground-based and Airborne Instrumentation for Astronomy IV, (2012).
- [7] Fata, R. G., Fabricant, D. G. "Design of a cell for the wide-field corrector for the converted MMT", Proc. SPIE 1998, Optomechanical Design, 32 (1993)
- [8] <http://www.bwc.com/products/components-accessories/dualvee.html>
- [9] Persson, S. E. ; Barkhouser, R. ; Birk, C. ; Hammond, R. ; Harding, A. ; Koch, E. R. ; Marshall, J. L. ; McCarthy, P. J. ; Murphy, D. ; Orndorff, J. ; Scharfstein, G. ; Shectman, S. A. ; Smee, S., Uomoto, A. "The FourStar infrared camera," Proc. SPIE 7014, Ground-based and Airborne Instrumentation for Astronomy II, (2008).
- [10] Smee, S. A., Barkhouser, R. H., Glazebrook, K. "Design of a multi-object high-throughput low-resolution fiber spectrograph for WFMOS," Proc. SPIE 6269, Ground-based and Airborne Instrumentation for Astronomy, (2006).
- [11] <http://www.bonn-shutter.de/>